Journal of Rock Mechanics and Geotechnical Engineering 8 (2016) 697–702

Contents lists available at ScienceDirect

Journal of Rock Mechanics and Geotechnical Engineering

journal homepage: www.rockgeotech.org

Full length article

Interaction analysis of back-to-back mechanically stabilized earth walls

Sadok Benmebarek*, Samir Attallaoui, Naïma Benmebarek

NMISSI Laboratory, Biskra University, Biskra 07000, Algeria

ARTICLE INFO

Article history:
Received 22 December 2015
Received in revised form
11 May 2016
Accepted 14 May 2016
Available online 15 July 2016

Keywords:
Back-to-back walls
Numerical analysis
Geosynthetic
Factor of safety
Lateral earth pressure
Maximum tensile force
Reinforcement

ABSTRACT

Back-to-back mechanically stabilized earth walls (BBMSEWs) are encountered in bridge approaches, ramp ways, rockfall protection systems, earth dams, levees and noise barriers. However, available design guidelines for BBMSEWs are limited and not applicable to numerical modeling when back-to-back walls interact with each other. The objective of this paper is to investigate, using PLAXIS code, the effects of the reduction in the distance between BBMSEW, the reinforcement length, the quality of backfill material and the connection of reinforcements in the middle, when the back-to-back walls are close. The results indicate that each of the BBMSEWs behaves independently if the width of the embankment between mechanically stabilized earth walls is greater than that of the active zone. This is in good agreement with the result of FHWA design guideline. However, the results show that the FHWA design guideline underestimates the lateral earth pressure when back-to-back walls interact with each other. Moreover, for closer BBMSEWs, FHWA design guideline strongly overestimates the maximum tensile force in the reinforcement. The investigation of the quality of backfill material shows that the minor increase in embankment cohesion can lead to significant reductions in both the lateral earth pressure and the maximum tensile force in geosynthetic. When the distance between the two earth walls is close to zero, the connection of reinforcement between back-to-back walls significantly improves the factor of safety.

1. Introduction

Mechanically stabilized earth (MSE) walls are well-recognized alternatives to conventional retaining walls due to many advantages such as ease of construction, economy, and aesthetics. For this, limit equilibrium and numerical methods were basically used to evaluate the stability of MSE walls (Leshchinsky and Han, 2004; Han and Leshchinsky, 2006, 2007, 2010). In recent years, back-to-back MSE walls (BBMSEWs) have been increasingly used for bridge approaches, ramp ways, rockfall protection systems, earth dams, levees and noise barriers. However, there are insufficient studies and guidelines concerning the behavior of BBMSEWs. FHWA design guideline (Berg et al., 2009) addressed the design of back-to-back walls, as illustrated in Fig. 1. Berg et al. (2009) divided back-to-back walls into two cases:

(1) Case 1: When the distance between the MSE walls, D, is greater than $H_1\tan(45^\circ - \varphi/2)$, where H_1 is the height of the higher wall and φ is the friction angle of the backfill, the width of the ramp or embankment allows for construction of two separate walls with sufficient spacing between them to ensure that each wall can act independently. Hence each wall can be designed individually.
(2) Case 2: When $D = 0$ and the overlap length exceeds $0.3H_2$, where H_2 is the height of the lower wall, two walls are still designed independently for internal stability but no active thrust to the reinforced zone is assumed from the backfill. In other words, no active earth thrust from the backfill needs to be considered for external stability analysis. In this case, the two walls are assumed to act as a whole, without backfill to exert an external destabilizing thrust.

For intermediate geometries between Cases 1 and 2, when $0 < D < H_1\tan(45^\circ - \varphi/2)$, Berg et al. (2009) suggested to interpolate linearly the earth pressure between full active earth pressure in Case 1 and zero earth pressure in Case 2. However, no justification was provided for this suggestion. Using numerical modeling

* Corresponding author. Tel.: +213 670071109.
E-mail address: sadok_benmebarek@yahoo.com (S. Benmebarek).
Peer review under responsibility of Institute of Rock and Soil Mechanics, Chinese Academy of Sciences.

http://dx.doi.org/10.1016/j.jrmge.2016.05.005

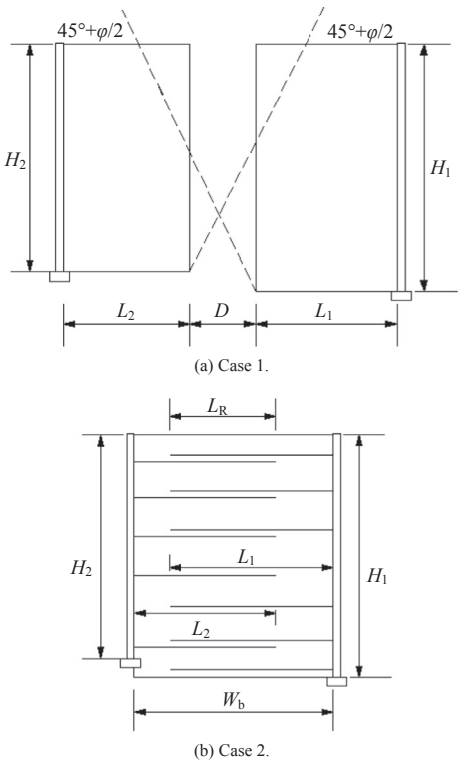

Fig. 1. Back-to-back mechanically stabilized earth walls (after Berg et al., 2009).

for the case of limit equilibrium state (i.e. the factor of safety $F_S = 1$), Han and Leshchinsky (2010) indicated that the FHWA design guideline underestimates the interaction distance, and for W/H_1 (W is the distance between two opposing wall facings) ranging from 2 to 3, the back-to-back walls still interact with each other. Recently, El-Sherbiny et al. (2013) analyzed different wall width to height ratios of BBMSEW using the finite element modeling. The numerical model was validated against an instrumented large-scale test wall (Won and Kim, 2007). It was indicated that when $D/H_1 < 1$, the two MSE walls interact with each other and the earth pressure behind the wall decreases because the failure wedge behind the wall is not fully developed.

In the above-mentioned studies, the interaction distance was identified when the critical failure surfaces in two opposing walls did not intercept each other. This seems to be not identical to that defined by the FHWA design guideline as shown in Fig. 1. In other words, a single failure surface may occur in one wall.

2. Numerical modeling

In this study, the PLAXIS software was utilized to perform the two-dimensional (2D) numerical analysis in the condition of plane strain. The geometry of the baseline model of BBMSEW (Fig. 2) considered in this study has the same configuration as that reported by Han and Leshchinsky (2010). The height of the walls is kept constant, equal to 6 m; and the soil foundation depth is equal to 2 m. The distance between the walls varies from $3H$ to $0.8H$ (large to narrow backfill width). Two soils are distinguished: backfill and base soils. The backfill material used for reinforced soil walls is assumed to be granular fill. A stiff soil like rock is chosen as the base soil to minimize its influence on the behavior of reinforced soil. The constitutive relation used for both soil types is the Mohr–Coulomb model. The properties of the two soils are shown in Table 1. The Tensar UX-1400 uniaxial geogrid was adopted to reinforce the BBMSEWs. The soils were simulated using 15-node triangular elements and the geogrid was modeled using an elastic-perfectly plastic model defined by the stiffness and tensile strength of geogrid. The vertical spacing of each layer of geogrid is 0.75 m. The length of reinforcement, $L = 4.2$ m, was selected to give $L/H = 0.7$. This ratio is the minimum value recommended by the FHWA design guideline for static design (Berg et al., 2009), except for Case 2 where $L/H = 0.6$ for the geometry with the overlap length, L_R, greater than $0.3H$. The geogrid properties used in modeling are summarized in Table 2. The well-known segmental precast concrete panels were considered in the current study to simulate the wall. Each wall contains 4 segmental concrete panels of 1.5 m in width and height and 0.14 m in thickness. The panels are modeled as a linear elastic material. For the panels, the Young's modulus $E = 25$ GPa, the Poisson's ratio $\nu = 0.2$, and the unit weight $\gamma = 23.5$ kN/m^3 Table 3 summarizes the panel properties as inputs to PLAXIS. The base of the wall is set to be hinged (i.e. the displacement of the wall is limited in vertical direction, but it is free to rotate and move in the horizontal direction).

In the numerical modeling, the geostatic stresses are firstly generated for the base soil. Secondly, the walls are constructed in stages, simulating the real construction process of these structures. The working stresses, strains, deformations, and tensile forces in the reinforcement are also evaluated in this phase. Then, reductions in φ and c (Brinkgreve et al., 2008) are conducted in models to determine the factor of safety. Finally, the methodology described above is validated by simulating the well-instrumented Founders/Meadow segmental bridge abutment reported by Abu-Hejleh et al. (2002).

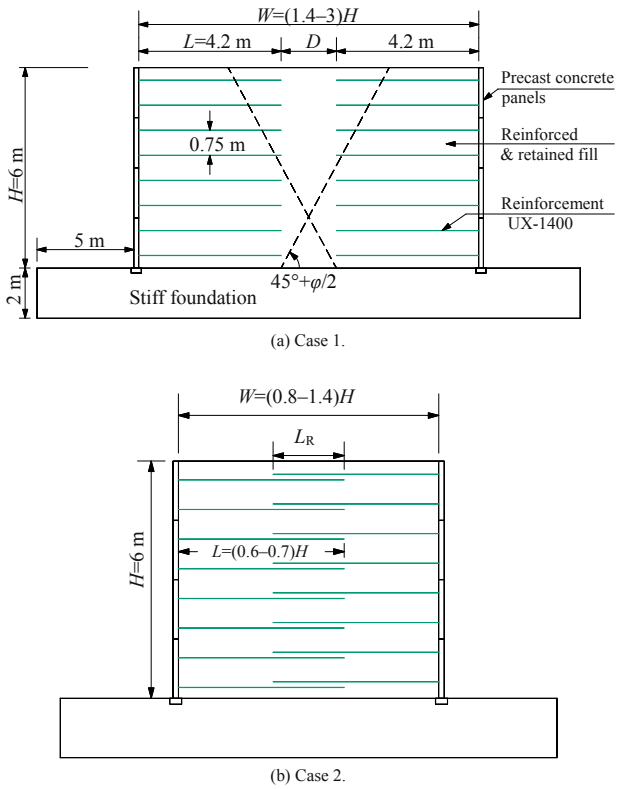

Fig. 2. Dimensions and parameters of the models.

Table 1
Material properties of backfill and base soil.

Model	Materials	Unit weight, γ (kN/m^3)	Friction angle, φ (°)	Dilation angle, ψ (°)	Cohesion, c (kPa)	Elastic modulus, E (MPa)	Poisson's ratio, ν
Elastic perfectly plastic Mohr–Coulomb	Backfill soil	18	30, 35, 40	5	0	30	0.3
	Base soil	22	30	0	100	200	0.2

Table 2
Properties of geosynthetic soil reinforcement.

Model	Ultimate tensile strength (kN/m)	Allowable tensile strength, T_a (kN/m)	Axial stiffness (kN/m)
Elastoplastic	70	25.6	1100

3. Computation results

3.1. Overall factor of safety

The factor of safety against shear failure was obtained using a shear strength reduction technique (Brinkgreve et al., 2008) for D values ranging from 0 to 1.6H ($W/H = 1.4$–3). The calculated factors of safety for Case 1 are presented in Fig. 3. The results are shown as the normalized distance between the back-to-back walls (D/H).

For soils with different friction angles ($\varphi = 40°$, 35° and 30°, as shown in Fig. 3), the factor of safety of the BBMSEW decreases firstly with the increase in the distance between the walls and then converges to a constant value, indicating the total attenuation of the interaction between two walls. For $\varphi = 40°$, 35° and 30°, the interaction distance D, based on the FHWA design guideline (Berg et al., 2009), as shown in Fig. 3, is found to be equal to 0.47H, 0.52H and 0.58H, respectively. It is clearly illustrated that the interaction distance obtained from the numerical analysis is smaller than that from the FHWA method. This is because that, in the FHWA method, the Rankine failure plane is assumed in the limit equilibrium state to determine the interaction between two back-to-back walls, while this study is based on a working stress and the failure planes are not formed in the numerical models when $F_S > 1.4$. This finding is different from Han and Leshchinsky (2010) based on the limit equilibrium state (i.e. $F_S = 1$). Decreasing D leads to the increase in the factor of safety for different friction angles.

Fig. 4 shows the factor of safety of back-to-back walls when $D \leq 0$ and the friction angle of backfill material $\varphi = 35°$. It is shown that the responses of the BBMSEW with overlapping and continuous reinforcements are different.

Table 3
Properties of facing panels (as input to PLAXIS).

Model	Axial stiffness, EA (kN/m)	Bending stiffness, EI (kN m^2/m)	Thickness, d (m)	Weight, w (kN m^{-2})	Poisson's ratio, ν
Elastic	3.5×10^6	5717	0.14	3.29	0.2

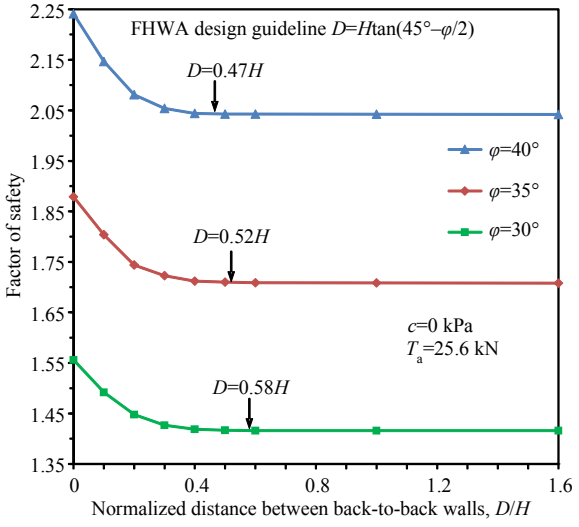

Fig. 3. Factor of safety of separate walls when $D \geq 0$ ($W/H = 1.4$–3).

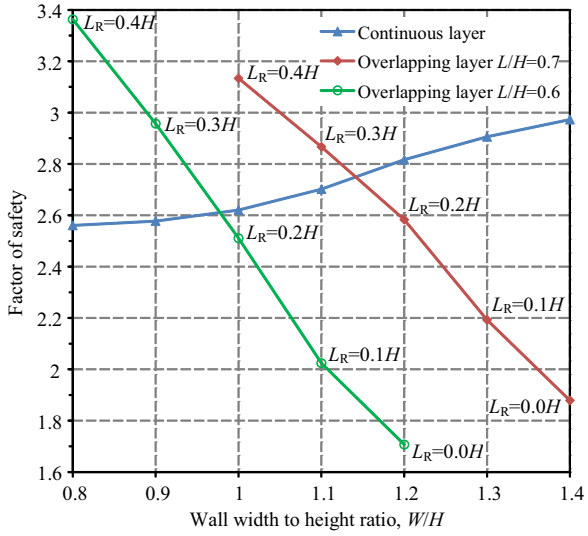

Fig. 4. Factor of safety of narrow walls when $D \leq 0$ ($W/H \leq 1.4$).

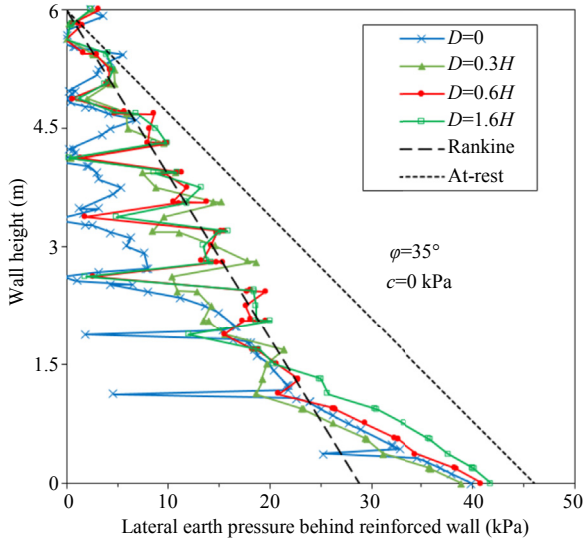

Fig. 5. Distribution of lateral earth pressure behind the reinforced wall.

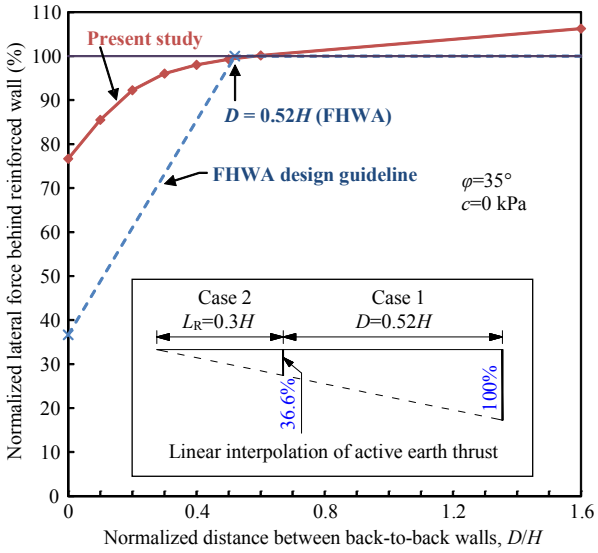

Fig. 6. Percentage of lateral thrust behind the reinforced wall.

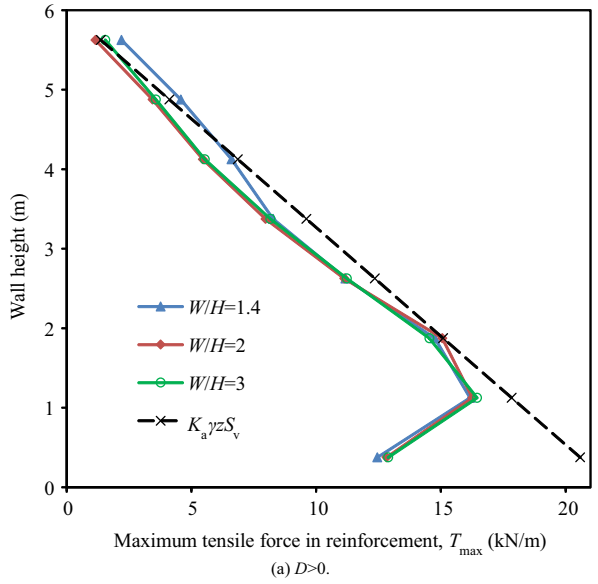

(a) $D>0$.

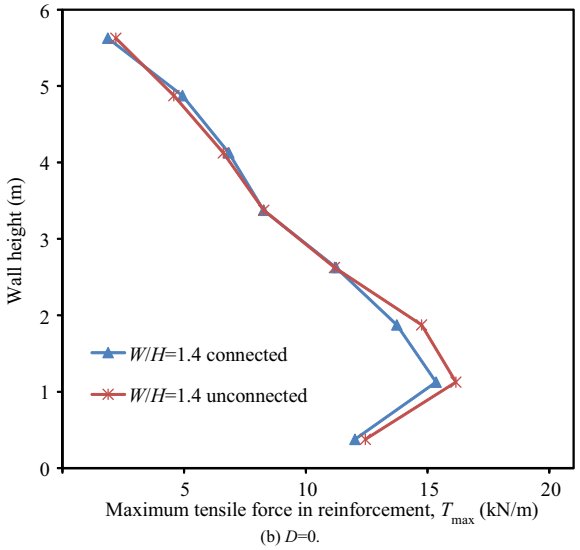

(b) $D=0$.

Fig. 7. Maximum tensile force in reinforcement at the end of construction.

For the case of $D = 0$, the comparison between connected and unconnected walls shows that the connection significantly improves the factor of safety. This can be explained by the fact that the pullout from the middle becomes impossible and each reinforcement can mobilize all its strength.

The factor of safety continues to increase with the decrease in the distance between the walls for the case of overlapping reinforcement. This is due to the increasing reinforcement overlapping length. However, for the case of walls with continuous layers of geogrid, the factor of safety slightly decreases with the decreasing W/H ratio. This may be related to the slight reduction in critical failure surfaces within walls. Furthermore, the decrease in the reinforcement length from $0.7H$ to $0.6H$, as suggested by FHWA design guideline (Berg et al., 2009) for Case 2, induces the decrease in the factor of safety.

3.2. Lateral earth pressure behind the reinforced wall

The lateral earth pressure behind the reinforced wall is presented in Fig. 5. The average lateral earth pressure behind the wall is close to the active Rankine lateral earth pressure when the value of D/H is large. Nevertheless, in the lower 1/4 of the wall, corresponding to the first precast segment, the lateral earth pressure increases and approaches the at-rest earth pressure. This is attributed to the restraint imposed at the base of the wall by the precast wall foundation, as clearly observed by wall displacements. Similar observations have been made from full-scale walls (Won and Kim, 2007; Huang et al., 2010). However, when the spacing D decreases from $1.6H$ to 0, the lateral earth pressure decreases. It is evident that the lateral earth pressure exists behind the reinforced wall even for $D = 0$.

The ratio of the active lateral thrust behind the reinforced wall to the theoretical active Rankine lateral thrust is presented in Fig. 6, which shows the influence of D/H on the mobilization of the lateral thrust. The lateral earth thrust exceeds the active Rankine earth thrust when D/H is greater than 0.6. This is related to the increase in lateral earth pressure at the wall base. Nevertheless, the lateral earth thrust evidently decreases when D is lower than $0.5H$. The lateral earth thrust decreases to 77% of the active Rankine lateral thrust as D approaches 0.

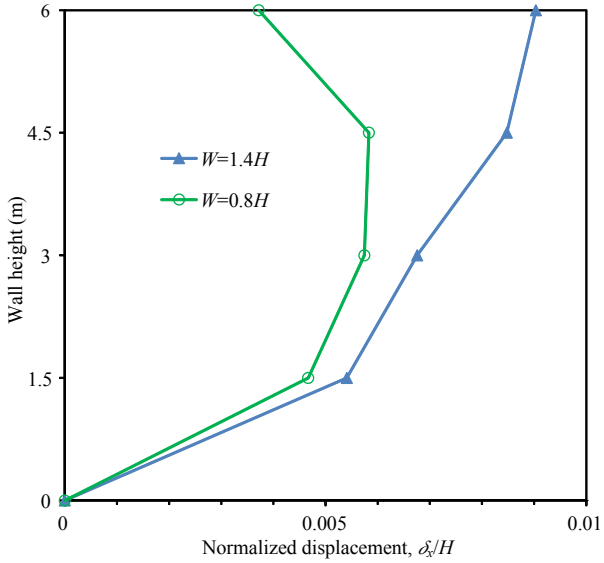

Fig. 8. Wall displacement at the end of construction.

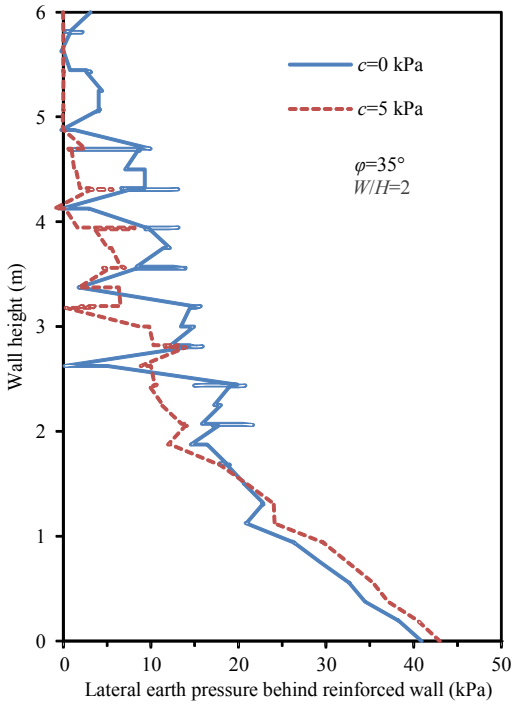

Fig. 9. Effect of cohesion on lateral earth pressure.

The comparison of the present numerical results to the values given by FHWA guideline (Berg et al., 2009), which suggested that the lateral earth pressure for external analysis should be ignored if $D = 0$ and the overlapping length exceeds $0.3H$, and that estimated by linear interpolation for D between 0 ($L_R = 0.3H$) and $0.52H$ shows that the pressure given by FHWA guideline (Berg et al., 2009) agrees well with the estimated one for Case 1, but for intermediate geometries between Cases 1 and 2, it is underestimated by FHWA guideline. For instance, when $D = 0$ and no connection exists, the active earth thrust obtained in the present study is 77% of the active Rankine lateral thrust, whilst the interpolation as suggested by FHWA gives 36.6%. A great value of lateral earth thrust (85% at $D = 0$) was also found by Han and Leshchinsky (2010).

3.3. Tensile force in the reinforcement

Soil reinforcement in MSE walls causes tensile forces to develop, which helps to stabilize the sliding mass of the wall. The tensile force developed in each layer of reinforcement is not uniform. The maximum tensile force in each layer of reinforcement obtained from the numerical analyses is presented in Fig. 7. For the case of $D > 0$ (Fig. 7a), the tensile forces in the reinforcement at different W/H ratios are found very close. The theoretical values for the normalized tensile force in each reinforcement layer using limit equilibrium methods based on Coulomb theory are also shown in Fig. 7a for comparison purpose based on the analyses of one wall, without consideration of wall interaction. These values are given by $K_a\gamma z S_v$ (Berg et al., 2009), where K_a is the active earth pressure coefficient, γ is the unit weight of the soil, z is the depth of reinforcement layer under consideration, and S_v is the vertical spacing between reinforcement layers. The computation results of tensile forces in the reinforcement for different W/H ratios covering Cases 1 and 2 of FHWA design guideline (Berg et al., 2009) match with the results obtained by the limit equilibrium method, which vary linearly with depth, except the lower quarter of the wall where the tensile force decreases due to the toe restraint at the base of the wall, as observed by Huang et al. (2010).

When $D = 0$ ($W/H = 1.4$), the tensile forces in the reinforcement (Fig. 7b) for both connected and unconnected walls are found very close. From the obtained results, we can conclude that the tensile forces in the reinforcement layers are lowly sensitive to the distance between the BBMSEWs. The limit equilibrium method can be used for computing the tensile forces with security for back-to-back

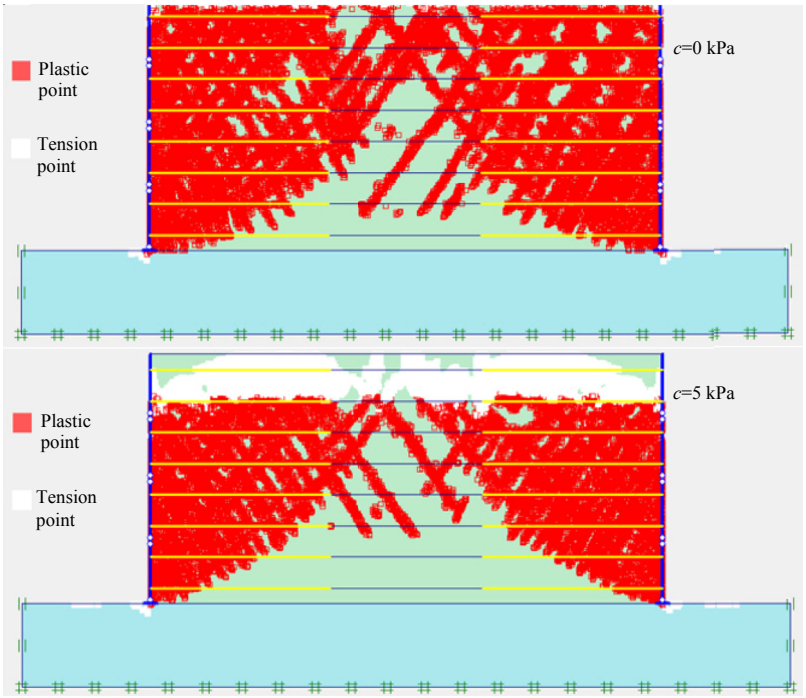

Fig. 10. Effect of cohesion within walls at $W/H = 2$.

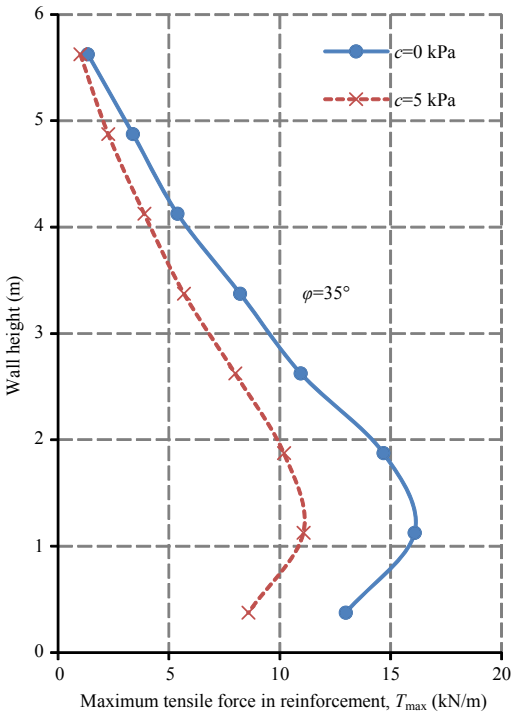

Fig. 11. Effect of cohesion on the maximum tensile force in geosynthetic.

stabilized retaining walls. The present computation results contradict those of the FHWA design guideline (Berg et al., 2009), which stated that the connected reinforcement creates an unyielding structure, developing an at-rest stress state (K_0) from the top to the bottom of the wall, resulting in much higher tensile forces in reinforcement than the FHWA design guideline (Berg et al., 2009). Berg et al. (2009) suggested that, to determine the tensile force in the reinforcement and connection, the increases in lateral stress must be considered in the design of facing elements. For closer BBMSEWs with multi-layer of geogrid running across the wall and for the case of overlapping reinforcement, the present computation results at $W/H = 1.4$ and 0.8 indicate that the wall's lateral displacements at the end of construction (Fig. 8) are more sufficient to develop the active earth pressure rather than the at-rest earth pressure.

3.4. Effect of cohesion

The effect of embankment cohesion is examined by increasing it from 0 to 5 kPa, which may cover practical values. As illustrated in Fig. 9, the lateral earth pressure behind the reinforced wall decreases with the increase in soil cohesion. It is observed that the lateral earth pressure at $c = 5$ kPa is equal to about zero at the top 1 m of the wall, as the cohesion greater than zero allows a tensile crack to develop at the wall top (Fig. 10).

It can be also seen from Fig. 11 that the maximum tensile force in geosynthetic decreases with the increase in soil cohesion at an average rate of 40%.

4. Conclusions

The finite element code PLAXIS was used to investigate the effect of the wall width to height ratio on internal and external stability of BBMSEW where the limit equilibrium method is rarely used. By comparison of computation results in this study with those of FHWA design guideline, the following conclusions can be drawn:

(1) The results of this study are consistent with those of FHWA design guideline that considers the significant interaction between the back-to-back walls when $D < H\tan(45^\circ - \varphi/2)$.
(2) The FHWA design guideline underestimates the lateral earth pressure when back-to-back walls interact with each other. The interaction is marked by both the decrease in the lateral earth pressure behind the reinforced wall and the increase in the factor of safety against shear failure.
(3) When D is close to zero, connection of reinforcement in back-to-back walls significantly improves the factor of safety.
(4) The maximum tensile force in reinforcement layers is nearly independent of the distance between the BBMSEWs even for very close walls. The maximum tensile force computed is found very close to that obtained by the limit equilibrium method. Thereby, for closer BBMSEWs, FHWA design guideline strongly overestimates the maximum tensile force.
(5) The results of this study indicate that a minor increase in embankment cohesion induces significant reductions in both lateral earth pressure and maximum tensile force in geogrid.

Conflict of interest

The authors wish to confirm that there are no known conflicts of interest associated with this publication and there has been no significant financial support for this work that could have influenced its outcome.

References

Abu-Hejleh N, Zornberg JG, Wang T, Watcharamonthein J. Monitored displacements of unique geosynthetic-reinforced soil bridge abutments. Geosynthetics International 2002;9(1):71–95.
Berg RR, Christopher BR, Samtani NC. Design and construction of mechanically stabilized earth walls and reinforced soil slopes – Volume 1. Publication No. FHWA-NHI-10–024. Washington, D.C.: U.S. Department of Transportation, Federal Highway Administration; 2009.
Brinkgreve R, Swolfs W, Engin E. PLAXIS finite element code. Delft, Netherlands: Delft University of Technology, PLAXIS bv; 2008.
El-Sherbiny R, Ibrahim E, Salem A. Stability of back-to-back mechanically stabilized earth walls. In: Proceedings of Geo-Congress 2013: Stability and Performance of Slopes and Embankments III. Reston, USA: American Society of Civil Engineers (ASCE); 2013. p. 555–65. http://dx.doi.org/10.1061/9780784412787.058.
Han J, Leshchinsky D. Analysis of back-to-back mechanically stabilized earth walls. Geotextiles and Geomembranes 2010;28(3):262–7.
Han J, Leshchinsky D. Stability analyses of geosynthetic-reinforced earth structures using limit equilibrium and numerical methods. In: Proceedings of the 8th International Conference on Geosynthetics (8ICG). Yokohama, Japan; 2006. p. 1347–50.
Han J, Leshchinsky D. Stability analysis of back-to-back MSE walls. In: Proceedings of the 5th International Symposium on Earth Reinforcement (IS Kyushu'07). Fukuoka: Japan; 2007. p. 487–90.
Huang B, Bathurst RJ, Hatami K, Allen TM. Influence of toe restraint on reinforced soil segmental walls. Canadian Geotechnical Journal 2010;47(8):885–904.
Leshchinsky D, Han J. Geosynthetic reinforced multitiered walls. Journal of Geotechnical and Geoenvironmental Engineering 2004;130(12):1225–35.
Won MS, Kim YS. Internal deformation behavior of geosynthetic-reinforced soil walls. Geotextiles and Geomembranes 2007;25(1):10–22.